† **Electronic Supplementary Information (ESI)**

Quasi-opsonin conjugated lipase-sensitive micelles activate macrophages against facultative intracellular bacterial infection†

1. Supplementary Methods

1.1 Synthesis of multifunctional block copolymers

Synthesis of B-mLBP, mLBP, B-cP and imP conjugates. 2-Chlorotrityl Chloride resin (0.4 mmol, 100~200 mesh, 1% DVB) was placed in a synthetic column and soaked in 15 mL DCM (dichloromethane) for 30 minutes until the resin was fully dissolved. Fmoc-protect amino acid dissolved in 15 mL of DCM was introduced into the reactor. After reaction under nitrogen agitation, the resin was washed three times with DMF (N, N-Dimethylformamide) and DCM (Dichloromethane). Then, 15 mL of deprotect solution (piperidine in DMF solution, V/V) was added to the obtained Fmoc-protected amino acid resin. Subsequently, Fmoc-amino acids-OH were reacted with the amino acids on the resin according to the order of amino acids from C-terminus to N-terminus in the expected polypeptide. After each condensation reaction, the resin was washed with DMF and methanol alternately. The resulted polypeptide was cleaved from the resin and purified by preparative HPLC. The purified solution was lyophilized to obtain the desired product (Scheme 1, (ii)). The solid-phase synthesis method of mLBP, B-cP, imP was consistent with B-mLBP. The only difference was the type and order of amino acids that undergo condensation reactions on the resin. According to the sequence of amino acids in the desired polypeptide, the condensation was performed from C-terminal to N-terminal in order to obtain mLBP, B-cP, and imP (mLBP: WKVRKSFFKLQGK, B-cP: KLVLRSKFRLQFK-biotin, imP: FHTRWNYWPYLH). The purity and molecular weight of the conjugates were confirmed by ESI-MS and HPLC.

Synthesis of Mal-PEG-PCL. The Mal-PEG-PCL block copolymers were synthesized by ring-opening polymerization of ε-CL in dry toluene under moisture-free high purity nitrogen atmosphere (Scheme 1, (i)). After cooling, the reaction mixture was dissolved in a minimal amount of CH_2Cl_2, and reprecipitated by dropwise addition to cold petroleum ether. Then the mixture was filtered before vacuum drying to attain constant weight. The chemical structures of the Mal-PEG-PCL was verified by ^{1}H NMR spectroscopy (300 MHz, d_6-DMSO) on a Bruker (AVANCE) III HD400 spectrometer.

Synthesis of B-mLBP-PEG-PCL, mLBP-PEG-PCL and B-cP-PEG-PCL. Mal-PEG-PCL was dissolved in acetone and this was added dropwise to pure water while stirring. The organic solvent was removed by rotating under reduced pressure. Then, mLBP, B-cP or B-mLBP was added in to react with Mal-PEG-PCL under stirring for 24 hours at room temperature. To remove unreacted polypeptide, dialysis (MWCO: 8000 Da) with pure water was conducted for 48 hours. The solution was collected and freeze-dried to obtain the desired product (Scheme 1, (iii)). The conjugation of mLBP, B-cP or B-mLBP with Mal-PEG-PCL was confirmed by HPLC performed on a Shimadzu system and ^{1}H NMR spectroscopy using Bruker (AVANCE) III HD400 spectrometer (300 MHz, d_6-DMSO).

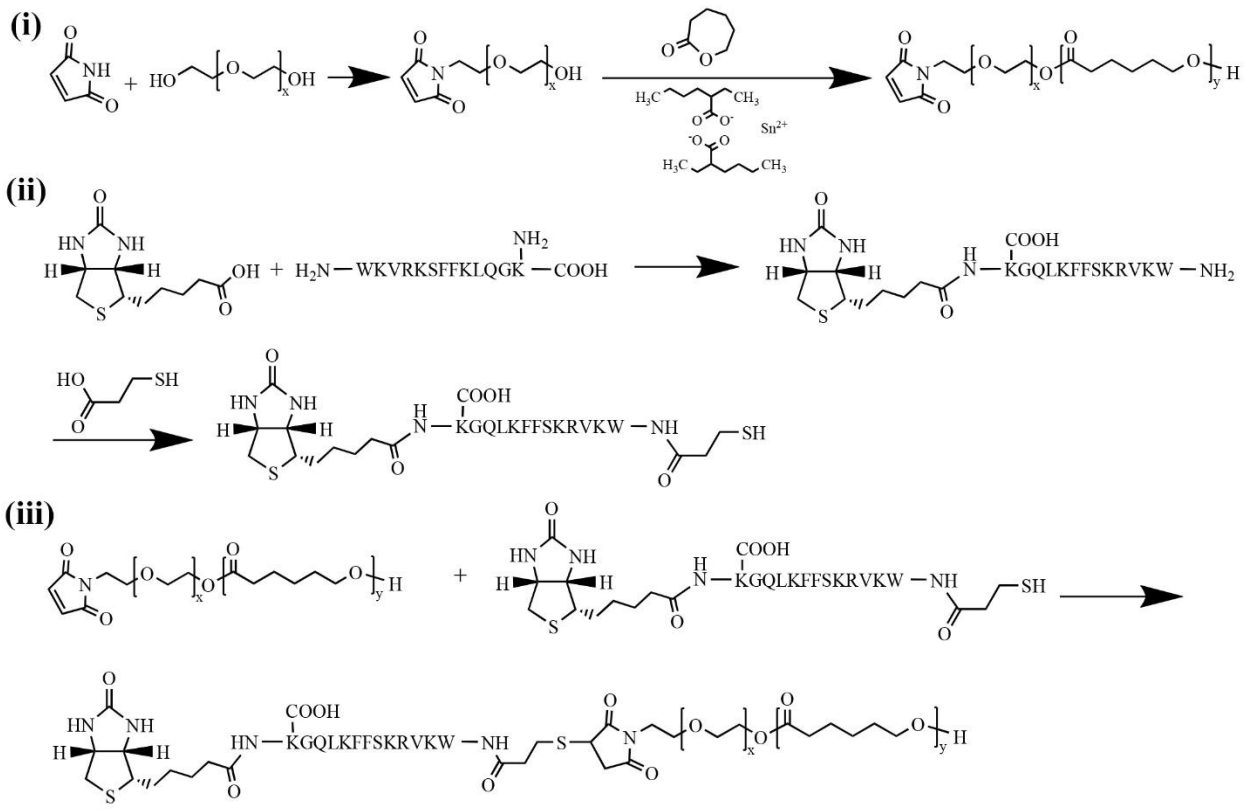

Scheme 1. Overall scheme for the synthesis of B-mLBP-PEG-PCL.

1.2 Interaction of B-mLBP, mLBP or cP with LPS

To investigate whether B-mLBP, mLBP or the reference materials cP (control peptide KLVLRSKFRLQFK with similar charge and solubility to mLBP) can interact with LPS, LPS (*E. coli* 0111: B4) was dissolved in 0.01 M PBS with a final concentration of 50 μM, and then incubated with 0.2 mmol/L B-mLBP, mLBP or cP at 37°C for 30 min, respectively. The PBS solution of B-mLBP, mLBP or cP (0.2 mmol/L) without LPS were set as the control groups. The secondary structure of these polypeptides before and after incubation with LPS was determined by circular dichroism spectrometer (optical path of quartz sample pool: 1 mm, sensitivity: 100 mdeg, time constant: 0.25 sec, wavelength range: 190-300 nm).

To further evaluate the interaction between B-mLBP, mLBP and LPS, the LPS-binding activity of B-mLBP and mLBP were measured by microscale thermophoresis using the NanoTemper Monolith NT.115 instrument set at Auto-detect Excitation Power and medium MST-Power. Each

measurement consists of 16 reaction mixtures in which the concentration of FITC-labelled B-mLBP or mLBP was set to be constant at 10 μM and the concentration of two fold-diluted LPS ranged from 25 μM to 0.75 nM. The MO. Affinity Analysis software was used to fit the data and to determine the K_d.

1.3 The quasi-opsonization of B-mLBP

Confocal microscopy was conducted to evaluate the quasi-opsonization effect of B-mLBP on *S.typhimurium* in the presence of macrophages. Bacteria were inactivated under high-pressure humid heat conditions (121°C, 20 min) to ensure the stability of labelled fluorescence while retaining their antigenicity. Then, the bacteria (3×10^8 CFU/mL) were incubated with 50 μg/mL fluorescein isothiocyanate (FITC) for 2 hours at 37°C. After washing with PBS three times, FITC-labelled *S.typhimurium* (FITC-Sal) were centrifuged for 10 min at 3000 rpm repeatedly until no free fluorescent dye was detected in the supernatant. Subsequently, FITC-Sal was re-suspended in culture medium and stored at 4°C for later use.

The cell-bound and phagocytosed bacteria were visualized using confocal microscopy (CLSM, LSM700, Carl Zeiss, Germany). Cells were incubated with 1 mL B-mLBP, B-cP, mLBP with FITC-Sal suspension obtained as described before for 8 hours at 37°C, 5% CO_2, respectively. Then the supernatant containing unbound bio-particle was removed. After the cells were washed with PBS for three times, 10 μg/mL Hoechst 33342 was added to stain the nucleus for 15 min. Then 200 μL of PBS solution was added in laser confocal petri dish after removing the stain, and the fluorescence images were then collected immediately.

1.4 The dual roles of B-mLBP

Screening for phagocytosis inhibitors. To screen out inhibitors that can effectively inhibit phagocytosis of bacteria by macrophages, 13 μg/mL of amiloride, 10 μg/mL of chlorpromazine, 54 μg/mL of flavonoids, and 0.25 mM N-ethylmaleimide (NEM) was added to pre-cultured RAW264.7 at 2×10^5 cells/mL and incubated for 30 min at 37°C. After discarding the supernatant and washing with PBS, FITC-Sal (green) was added to a petri dish and incubated at 37°C. After 4 h, Hoechst 33342 was used to stain the nucleus of macrophages (blue).

To screening the incubation concentration of NEM, 0.20 mM and 0.10 mM of NEM were added to pre-cultured RAW264.7 at 2×10^5 cells/mL and incubated for 30 min at 37°C. After discarding the supernatant and washing with PBS, FITC-Sal (green) was added to a petri dish and incubated for 4 h. The nucleus was stained blue by Hoechst 33342.

To screening the incubation time of NEM, 0.10 mM of NEM was added to pre-cultured RAW264.7 (2×10^5 cells/mL) and incubated for 30, 15, 5 min at 37°C, respectively. After discarding the supernatant and washing with PBS, the cells were incubated with FITC-Sal (green) for 4 h and the nuclei were stained by Hoechst 33342 (blue).

The RAW264.7 cells were seeded in a laser confocal petri dish at a concentration of 2×10^5 cells/mL and allowed to grow in a humidified atmosphere containing 5% CO_2 at 37°C. After 8 hours, the medium was removed and then incubated with the appropriate dye or samples for each specific experiment as listed below.

The quasi-opsonization mechanism of B-mLBP. To investigate the quasi-opsonization mechanism of the material, their stimulative bacteria-binding and phagocytosis by macrophage were inspected separately. At first, the phagocytosis was inhibited with N-ethylmaleimide (NEM) (0.10 mM), a chemical inhibitor of phagocytosis, for 10 min followed by the addition of samples to find out the functional group that affects bacteria-binding by the macrophage. NEM inhibits oxidative metabolism associated with phagocytosis by inhibiting -SH groups inside and outside the cell membrane. The pre-treated cells were incubated with 1 mL of B-mLBP, B-cP, mLBP with FITC-Sal suspension for 8 hours at 37°C, 5% CO_2, respectively. The medium in each well was removed and Hoechst 33342 was added at a final concentration of 10 μg/mL to stain the nucleus for 15 min. Cells were then washed three times with 0.01 M PBS before observation.

Secondly, trypan blue which cannot enter living cells was used to quench fluorescence on the surface of cell membranes or extracellularly to verify the functional group that affects phagocytosis. After the cells were incubated with 1 mL of B-mLBP, B-cP, mLBP with FITC-Sal suspension at 37°C, 5% CO_2 for 8 hours, supernatant was discarded and 0.125% trypan blue was added to incubate for 10 min. After washed, 10 μg/mL Hoechst 33342 was added to the cells to stain the nucleus for 15 min. Cells were then washed three times with 0.01 M PBS before observation.

For the flow cytometry test, RAW264.7 cell monolayers were harvested and seeded in 24-well plates at a concentration of 2 ×10^5 cells/well for 8 hours. For experiments, B-mLBP, B-cP, and mLBP with a final concentration of 2 mg/mL were dissolved in the FITC-Sal suspension and added to the 24-well plate at 0.5 mL per well. At certain time intervals (1, 2, 4, 8 hours), excess bacteria were removed by multiple washes with 0.01 M PBS and centrifugation at 1000 rpm, 3 min. Cell monolayers were harvested in the form of a single cell suspension. A fluorescence-activated cell sorter (FACScan, Becton Dickinson Immunocytometry Systems, Mountain View, CA) was used to measure individual cells for green fluorescence. 10^4 cells were measured in each sample. Gates were set on RAW264.7 cells during measurement to exclude cell debris and dissociative bacteria.

1.5 Regulatory effect of synthetic peptides on inflammation

The regulatory effect of synthetic peptides on inflammation-related factors secreted by macrophages was examined by ELISA. After the cells were cultured in the 96-well plate for 12 hours, the medium was discarded, and 200 μL of fresh medium containing each polypeptide (0.2 μM B-mLBP, mLBP, B-cP, imP (Inflammatory peptide)) and LPS (1 μg/mL) was added. Cells and cells with LPS only were used as control groups. Each experimental group was set with sampling holes at different time points of 6, 12, 24, 36, 48 hours, respectively. At the predetermined time point, the supernatant medium was transferred to a 2 mL EP tube and stored at -80°C. The TNF-α, IL-6 and IL-10 phagocytosis-related cytokines in the supernatant were detected according to the instructions of the ELISA kit.

1.6 Induction of chloramphenicol-resistant *S.typhimurium*

The MIC before and after induction was determined by the broth microdilution method. In brief, chloramphenicol solutions with different concentrations after doubling dilution were added to sterilized 96-well enzyme standard plates, respectively. 50 μL of bacterial solution (1.5×10^5 CFU/mL) was added in each well and incubate at 37°C for 18 h. A well containing only bacteria was used as a positive control well, and a well containing only a drug solution was used as a negative control. The concentration of the drug corresponding to the well that completely

(100%) inhibited the growth of bacteria was taken as MIC. After the MIC was determined, the Salmonella culture was inoculated on a medium containing the drug with 1/2-fold MIC, and cultured at 37°C for 24 h. Subsequently, the well-grown strain was inoculated on a medium containing 1-fold MIC of the drug and continued to be cultured for 24 h, until it was inoculated on a medium containing 128-fold MIC of the drug. The induced strains were subcultured 4 times without induction, and the MIC was measured.

1.7 Effect of bacterial concentration on macrophage activity

Bacterial suspensions (2×10^5, 5×10^5, 2×10^6, 5×10^6, 2×10^7, 5×10^7, 2×10^8 CFU/mL) were added to precultured RAW 264.7 cells in 96-well plates. After 8 h, the supernatant was discarded and washed three times with 0.01 M PBS to remove residual bacteria. The cells were pipetted down with medium to obtain cell suspensions. After diluting the suspensions to 1 mL with the medium, 20 μL of the suspension was pipetted onto a cell counting plate for counting.

1.8 Establishment of a localized *S.typhimurium* infection model of thigh

The *S.typhimurium* (10^7 CFU/mL), dispersed in 0.1% agar suspension, was subcutaneously injected into each thigh of mice, and then the survival status of mice for 3 days was recorded. After 3 days, the medial part of thigh was dissected to identify the inoculation of *S.typhimurium* in thigh tissue of mice. Moreover, the blood was also taken from orbit to guarantee no systemic infection.

1.9 Establishment of an acute intraperitoneal *S.typhimurium* infection model

The Minimum Lethal Dose (MLD) of *S.typhimurium* was determined to be 4.2×10^6 CFU/mL. And then, the *S.typhimurium*, dispersed in saline suspension containing 5% gastrin, was injected into the abdominal cavity of mice to establish the acute intraperitoneal *S.typhimurium* infection model.

2. Supplementary results and discussion

2.1 Synthesis of multifunctional block copolymers

To prove our conjecture, B-mLBP and the reference materials B-cP (Biotin grafting control peptide KLVLRSKFRLQFK with similar charge and solubility to mLBP) and mLBP were synthesized and characterized by ESI-MS and HPLC. Based on the excimer ion peak [M+4H]4+ with a mass-to-charge ratio of 470.6 m/z and the excimer ion peak [M+3H]3+ with a mass-to-charge ratio of 626.8 m/z, the relative molecular weight of B-mLBP was about 1877, which was in line with expected values (Figure S1A, ESI †). According to the HPLC spectrum, the purity of prepared product was 99.32% (Figure S1B, ESI †). The characterization data of mLBP and B-cP are shown in Figure S2A, B and Figure S3A, B (ESI †).

Later the B-mLBP was conjugated with a lipase-sensitive block PEG-PCL. Maleimide-PEG-PCL (Mal-PEG-PCL) was firstly synthesized and verified by ^{1}H NMR spectroscopy (Figure S1D, ESI †). Seen from the ^{1}H NMR spectrum, the peak at 6.69 ppm proved the conjugation between Mal group and PEG segments. The corresponding peaks at 1.38, 1.65, 2.31, 4.06 (CH_2 in PCL), 3.64 (CH_2 in PEG) ppm reflected the addition of caprolactone to PEG with ring-opening. The conjugation of B-mLBP with Mal-PEG-PCL was confirmed by HPLC and ^{1}H NMR. The mixture of B-mLBP and Mal-PEG-PCL exhibited an absorption peak belonging to B-mLBP at 12.56 min before reaction. As the reaction went on, the absorption peak at 12.56 min gradually decreased and eventually disappeared at 12 h, which could be one of evidence of the formation of B-mLBP-PEG-PCL (Figure S1C in red dotted box, ESI †). For the ^{1}H NMR spectrum of B-mLBP-PEG-PCL, the main corresponding signals at 1.29, 1.53, 2.28, 3.98 (CH_2 in PCL), 3.51 (CH_2 in PEG) ppm confirmed the existence of PEG-PCL blocks in the synthesized product. The peak at 6.68 ppm indicated the conjugation between the Mal group of Mal-PEG-PCL and the thiol group of B-mLBP. In addition, a series of signal peaks between 6.76 and 8.50 ppm can be attributed to the amino acids in mLBP, which also verified the coupling of B-mLBP with PEG-PCL (Figure S1D, ESI †). The characterization data of the control block materials mLBP-PEG-PCL, B-cP-PEG-PCL, and PEG-PCL are shown in Figure S2C and Figure S3C (ESI †).

2.2 Interaction of B-mLBP, mLBP or cP with LPS

Circular dichroism detection was conducted to verify that mLBP can target adhere to the surface of bacteria, in which LPS, a major component in the outer membrane of Gram-negative bacteria, was employed (Figure S5A and Figure S5B, ESI †). Compared with free B-mLBP, the α-helix and β-fold structures of B-mLBP increased by 4.7% and 66.7% after mixing with LPS, while the β-turn and random coil structure reduced by 32.9% and 38.4%, respectively, representing the interaction of LPS with B-mLBP. As for the mixed mLBP, the change in β-fold, random coil and β-turn structures also suggested the interaction of LPS with mLBP. However, for B-cP, there was no significant change in the secondary structure before and after mixing with LPS. Therefore, mLBP was the main component responsible for binding with LPS. The difference in secondary structure between mLBP and B-mLBP after mixing with LPS may result from the special influence of biotin conjugated in mLBP. As shown in Figure S5C and Figure S5D (ESI †), B-mLBP and mLBP could bind with LPS, the K_d of B-mLBP and LPS measured by microscale thermophoresis was 0.606 μM, and the K_d of mLBP and LPS measured was 0.324 μM. The binding ability between mLBP and LPS was even stronger than that between B-mLBP and LPS, which may be due to the difference of steric hindrance caused by conjugated biotin.

2.3 The quasi-opsonization of B-mLBP

In a proof-of-concept study, laser confocal imaging was performed to visualize the phagocytosis behavior of macrophages in the presence of bacteria and different conjugates. Seen from Figure S5E (ESI †), the B-mLBP group exhibited the highest bacterial adhesion and endocytosis with strong fluorescence both inside and outside cells. Compared to B-cP which exhibited clusters of fluorescence intracellularly, most of the bacterial fluorescence in mLBP group appeared on the surface of macrophages. Thus, mLBP may contribute to bacterial adhesion and act as a linker to gather more bacteria available for phagocytosis. Biotin is responsible for enhancing the phagocytosis of macrophages. When conjugating biotin and mLBP together, B-mLBP could exert synergism of these two function groups, thus exhibiting quasi-opsonization similar to natural LBP.

2.4 The dual roles of B-mLBP

To further confirm the binding and phagocytosis promoting roles of B-mLBP, phagocytic inhibitor,[1, 2] and trypan blue dye[3] were used to inhibit macrophage phagocytosis and quench the fluorescence on the surface of macrophage membrane or in the medium, respectively. After the phagocytosis of RAW264.7 was inhibited by incubating with 0.1 mM NEM for 5 min (Figure S6A-C, ESI †), the FITC fluorescence intensity on the cell membrane surface in the presence of B-mLBP and mLBP was equally strong, indicating that the biotin motif barely contributed to the bacterial binding. Without mLBP motif, little fluorescence intensity was observed in the B-cP group, which was similar to that of blank groups, suggesting the prerequisite role of bacterial adherence by mLBP in promoting phagocytosis to macrophages (Figure S7, ESI †). After the extracellular fluorescence was quenched, B-mLBP exhibited much stronger mean fluorescence intensity (MFI) than mLBP, mostly intracellularly, indicating that biotin could further promote bacteria phagocytosis. The stronger MFI of the mLBP group than the blank group was probably attributed to the promoted adhesion between bacteria and macrophages (Figure S8, ESI †), facilitating the natural phagocytosis. Besides, in the flow cytometry analysis which could be considered as quantification of FITC-labelled *S.typhimurium* (FITC-Sal) phagocytosed by macrophages,[4] the MFI of FITC in each peptide group at each time point all increased and the order of MFI was B-mLBP> B-cP> mLBP, reaffirming the above inference (Figure S9A and Figure S9B, ESI †).

2.5 Regulatory effect of synthetic peptides on inflammation

Immune cells could promote the digestion of invading pathogens by producing pro-inflammatory factors such as TNF-α and IL-6,[5] which are usually accompanied with tissue injury. Accordingly, the regulatory effect of such quasi-opsonization materials on inflammatory factors needs to be considered to investigate their safety and effectiveness for combined antibacterial (Figure S10, ESI †). The imP which was confirmed to up-regulate pro-inflammatory factors,[6] has been synthesized (Figure S4A and Figure S4B, ESI †) and used as a positive control peptide. For the mLBP and imP groups, the TNF-α pro-inflammatory factor continued to increase and remained high, while the expression of anti-inflammatory factor IL-10 was

inhibited, which indicated an uncontrolled immune response. In the B-cP group, the expressions of TNF-α, IL-6 and IL-10 all increased rapidly and then decreased. However, after a transiently decline, the expression of TNF-α was up-regulated again, causing the overexpression of inflammatory factors. In contrast, in the B-mLBP group, macrophages could rapidly up-regulate the expression of TNF-α and IL-6, thus could increase phagocytose of LPS in response as proved in Figure S5E (ESI †). Meanwhile, the IL-10 was also strongly expressed, controlling the over-expression of TNF-α and IL-6, which decreased rapidly after 6 h. In turn, the decrease of TNF-α and IL-6 served as a feedback signal to gradually reduce the expression of IL-10. The balance between pro-inflammatory and anti-inflammatory responses not only improved the immune phagocytosis of macrophages, but may also maintained the relative homeostasis *in vivo*. Therefore, B-mLBP was adopted as a safe and functional ligand for drug delivery system in our subsequent studies.

3. Supplementary Figures

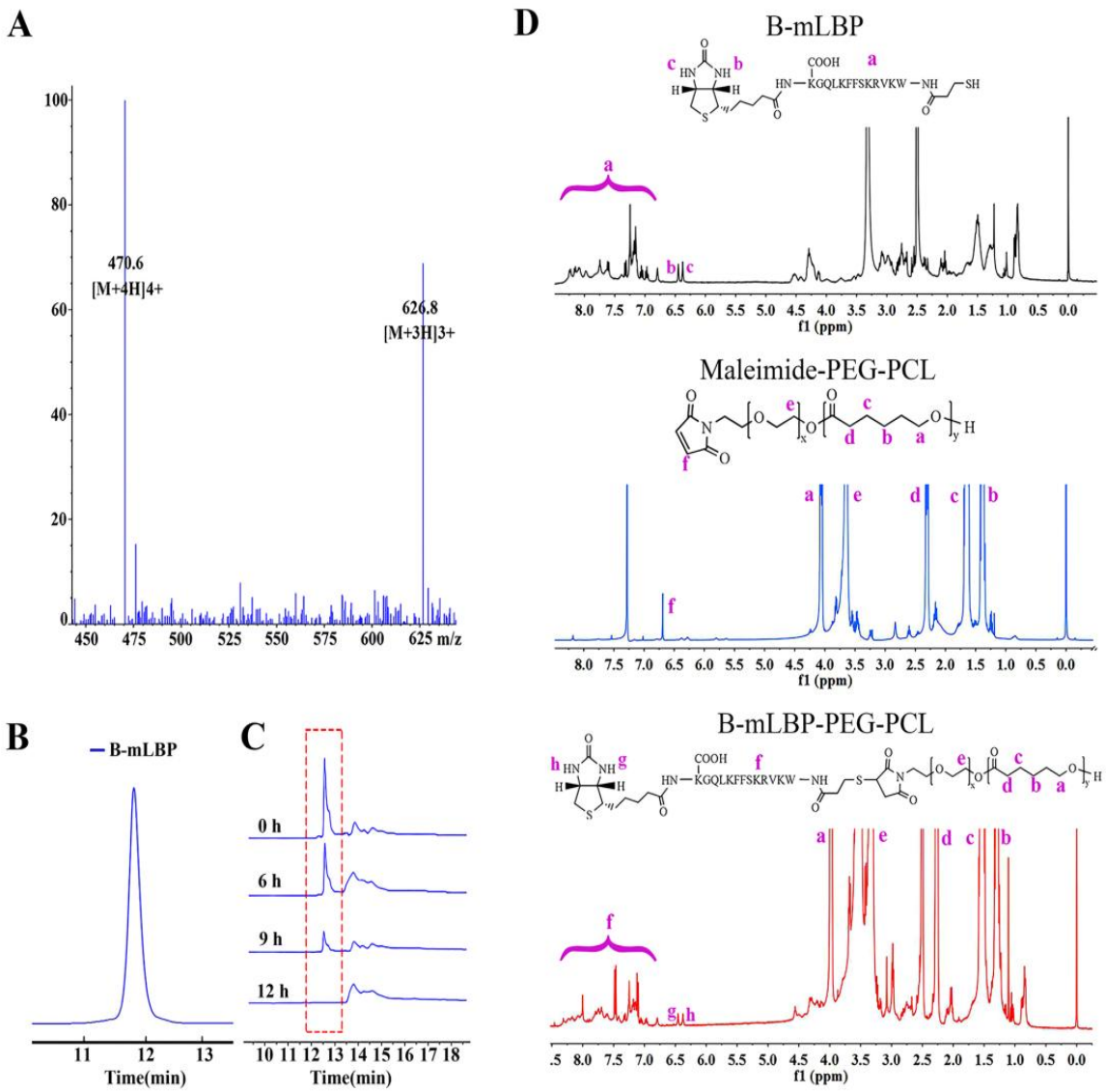

Figure S1. Synthesis and identification of multifunctional block copolymers B-mLBP. (A) ESI-MS spectrum of B-mLBP (B) The HPLC spectrum of B-mLBP (C) The HPLC spectrum of the reaction system of B-mLBP and Maleimide-PEG-PCL at different time points (0, 6, 9, 12 hours). (D) ^{1}H NMR spectra of Maleimide-PEG-PCL, B-mLBP, and B-mLBP-PEG-PCL in DMSO.

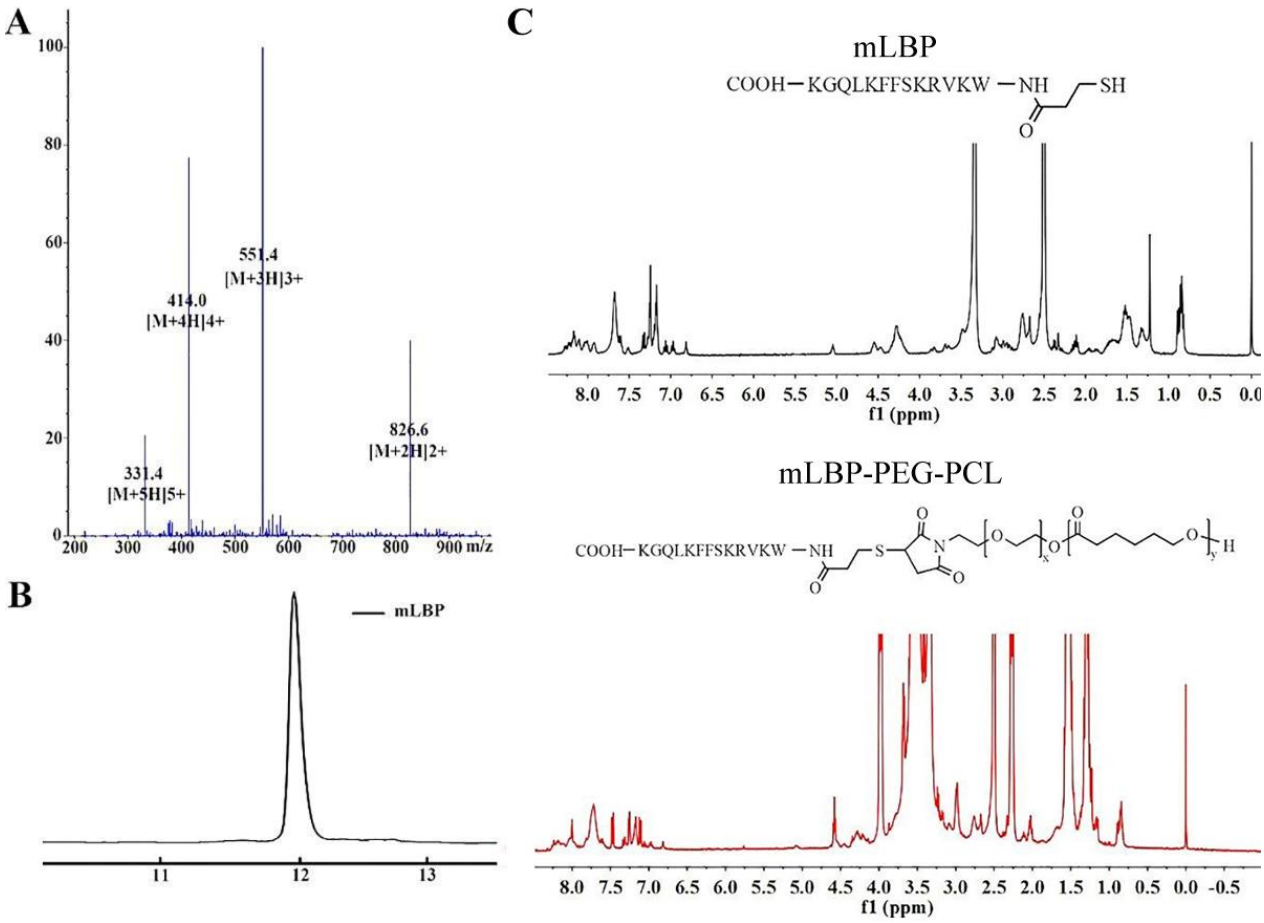

Figure S2. Synthesis and identification of mLBP. (A) ESI-MS spectrum of mLBP (B) The HPLC spectrum of mLBP (C) ^{1}H NMR spectra of mLBP, and mLBP-PEG-PCL in DMSO.

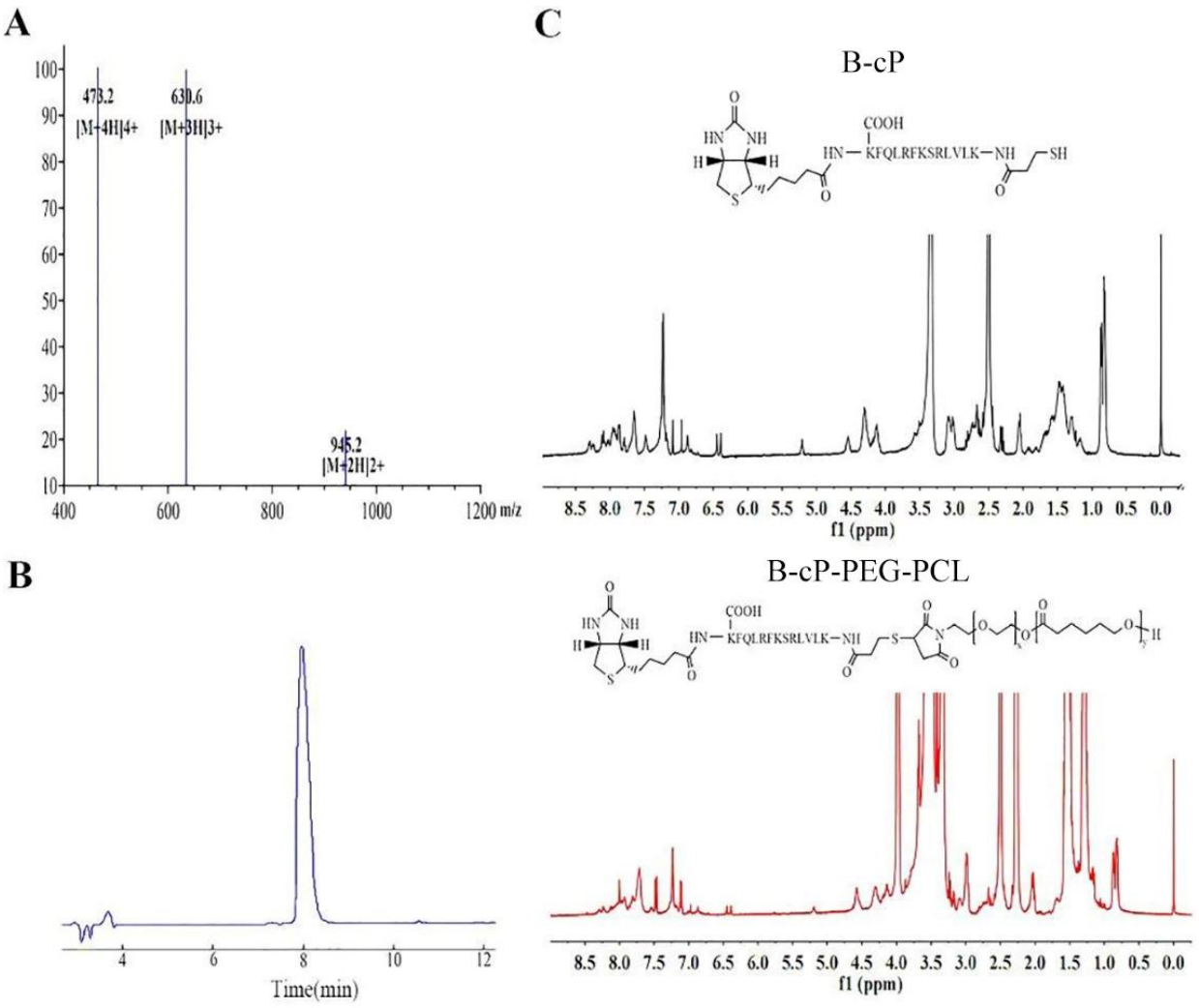

Figure S3. Synthesis and identification of B-cP. (A) ESI-MS spectrum of B-cP (B) The HPLC spectrum of B-cP (C) ^{1}H NMR spectra of B-cP and B-cP-PEG-PCL in DMSO.

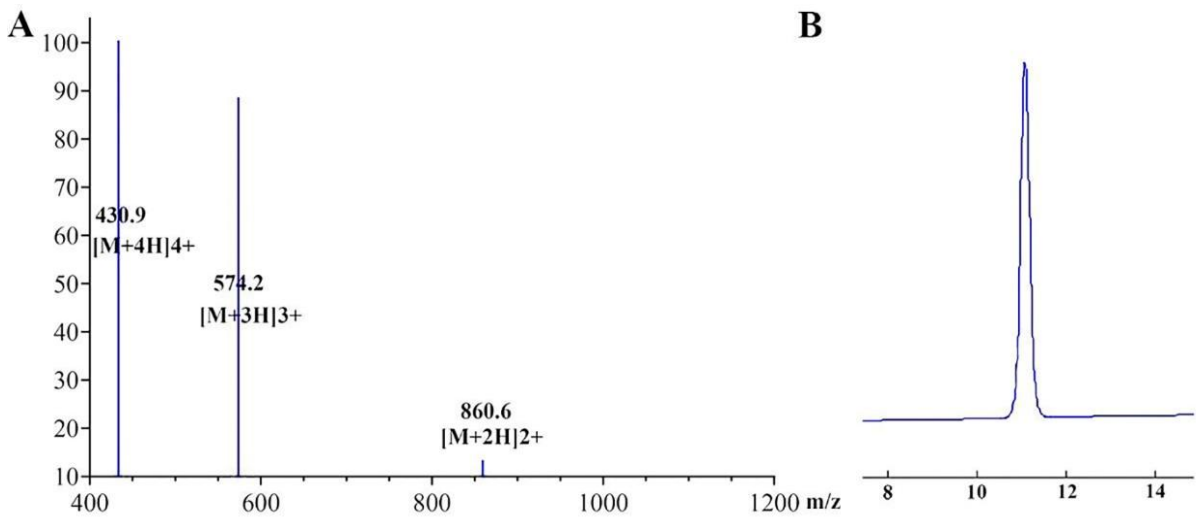

Figure S4. Synthesis and identification of imP. ESI-MS (B) and HPLC (A) spectrum of Inflammatory related mimic peptide (imP).

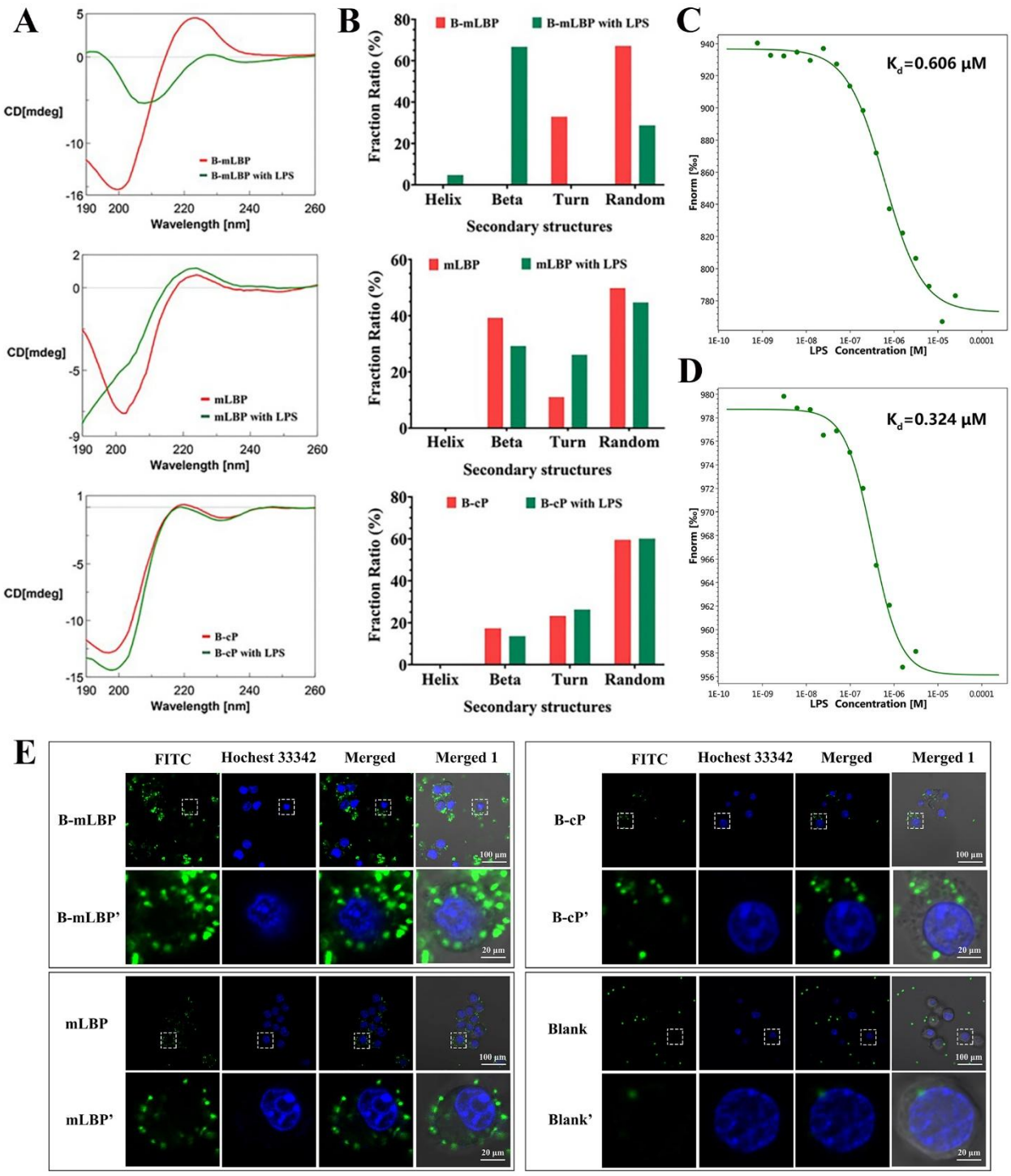

Figure S5. Interaction of B-mLBP, mLBP or cP with LPS and the quasi-opsonization of B-mLBP. (A) Circular dichroism spectrum of B-mLBP, mLBP, B-cP in the absence or presence of 50 μM LPS. (B) The secondary structure ratio of B-mLBP, mLBP, B-cP in the absence or presence of 50 μM LPS. The binding of LPS by B-mLBP (C) and mLBP (D). Binding of LPS by FITC labelled B-mLBP and mLBP was evaluated using microscale thermophoresis in which the concentration of B-mLBP or mLBP was kept constant. K_d was determined by the

MO. Affinity Analysis software. (E) Fluorescent microscopy images of RAW264.7 stained with DAPI to nuclei (blue signal) after incubation with B-mLBP, mLBP, B-cP, cell culture medium (Blank) in the presence of FITC-Sal (green signal) at 37°C for 8 h. B-mLBP', mLBP', B-cP' or Blank' represents the enlarged image in white dotted box of B-mLBP, mLBP, B-cP, or Blank group.

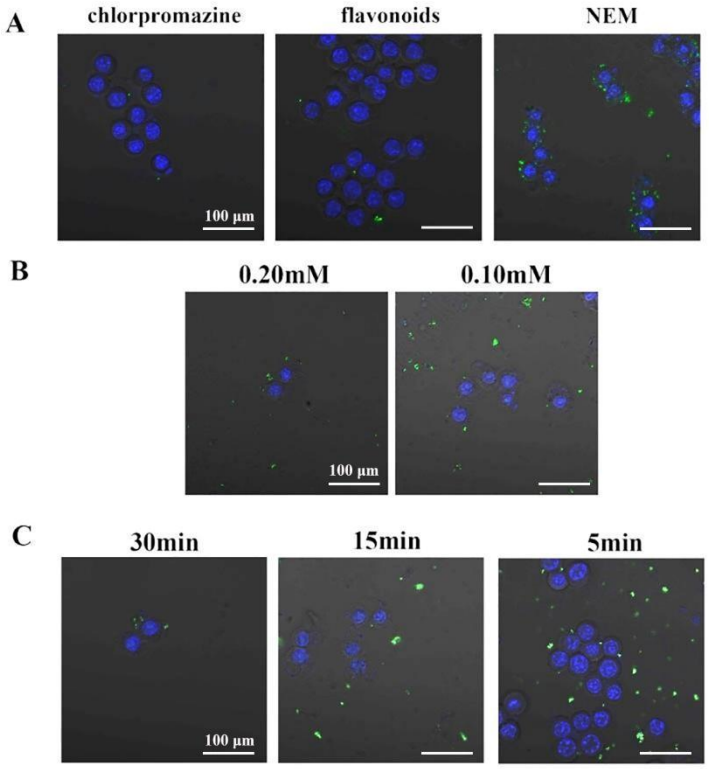

Figure S6. Screening of phagocytic inhibitors and treatment conditions. (A) Laser confocal imaging for screening the type of phagocytic inhibitors. (B) Laser confocal imaging for screening the incubation concentration of NEM. (C) Laser confocal imaging for screening the incubation time of NEM.

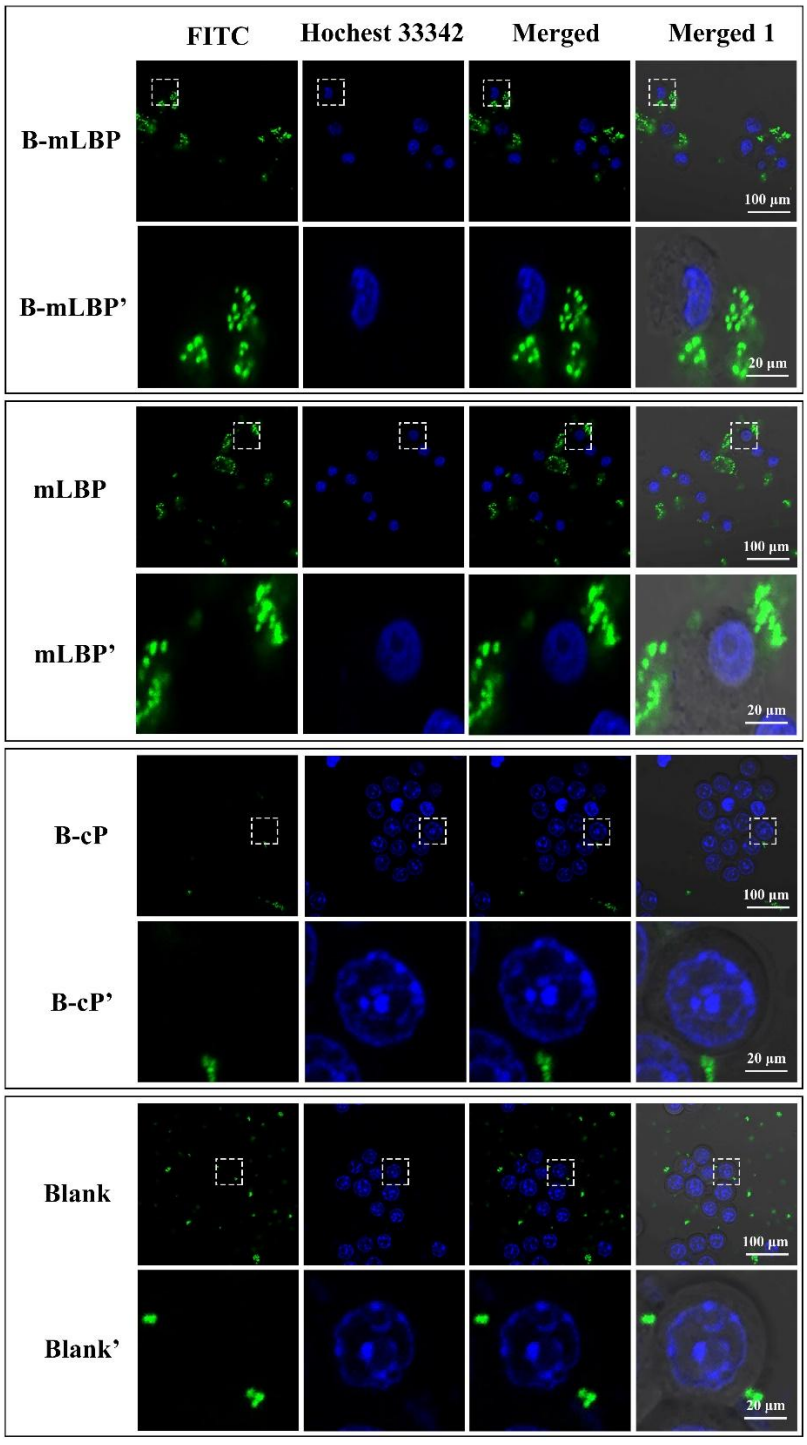

Figure S7. Fluorescent microscopy images of RAW264.7 pretreated with NEM phagocytosis inhibitor after incubation with B-mLBP, mLBP, B-cP, cell culture medium (Blank) in the presence of FITC-Sal (green signal) at 37°C for 8 h. B-mLBP', mLBP', B-cP' or Blank' represents the enlarged image in white dotted box of B-mLBP, mLBP, B-cP, or Blank group.

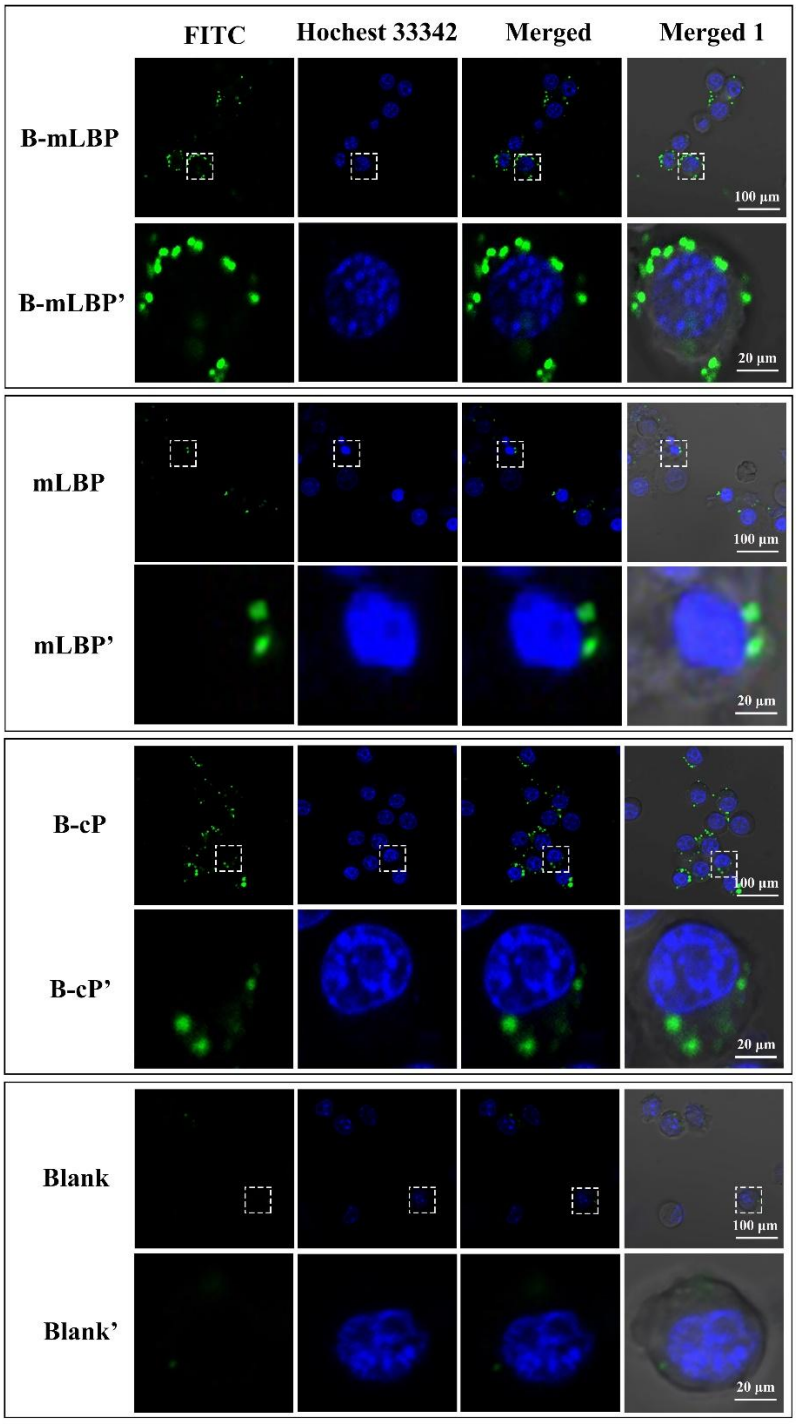

Figure S8. Fluorescent microscopy images of the internalized FITC-Sal by RAW264.7 (nuclear, blue signal) after incubation with B-mLBP, mLBP, B-cP, cell culture medium (Blank) in the presence of FITC-Sal (green signal) at 37°C for 8 h. Trypan blue was added to quench fluorescence on the cell surface and extracellularly before observation. B-mLBP', mLBP', B-cP' or Blank' represents the enlarged image in white dotted box of B-mLBP, mLBP, B-cP, or Blank group.

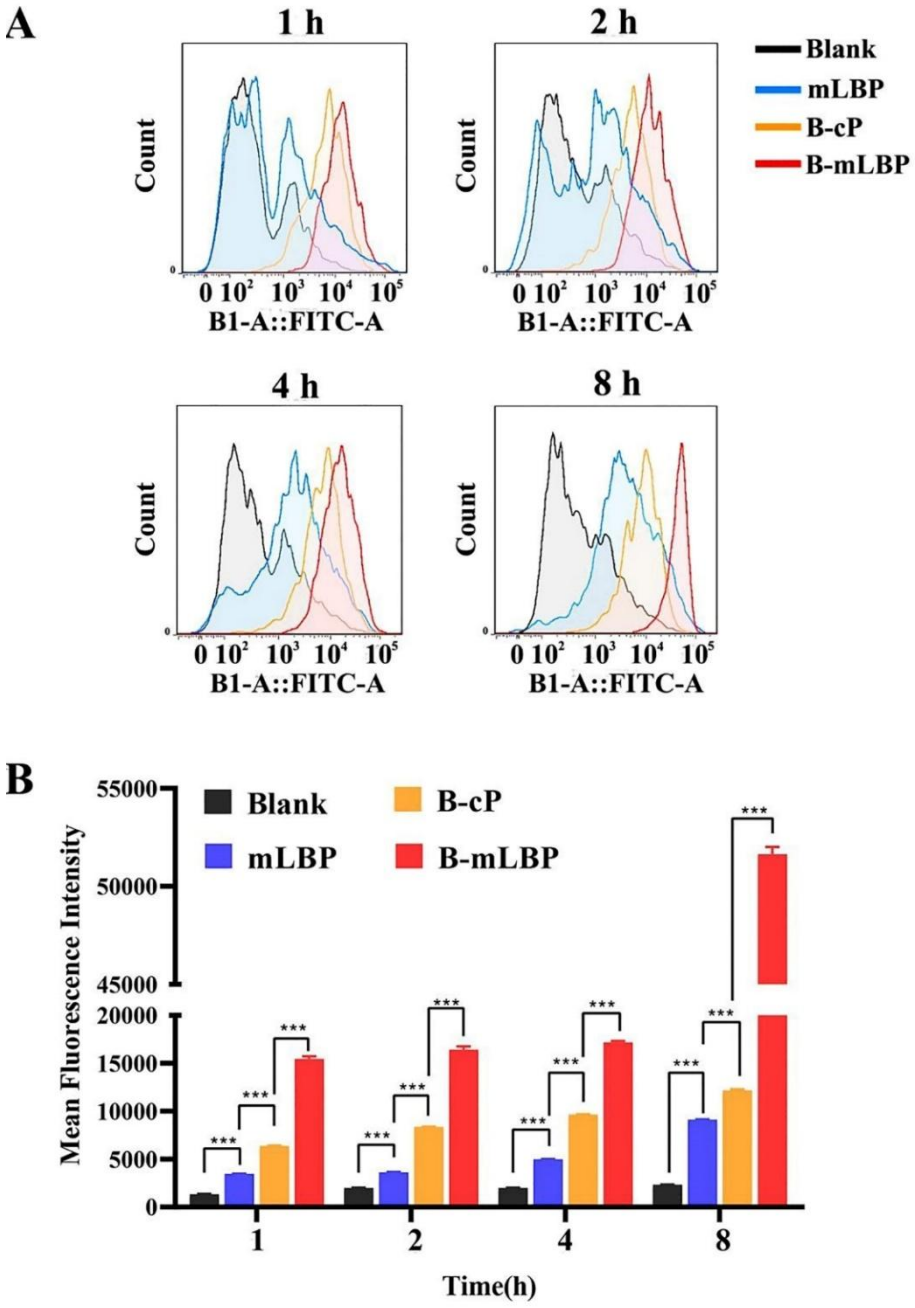

Figure S9. Flow cytometry (A) and histogram (B) displayed the relative FITC fluorescence intensity of the internalized FITC-Sal in RAW264.7 treated with cell culture medium (Blank), mLBP, B-cP, or B-mLBP, respectively, at different time points (1, 2, 4, 8 h) (n=3). *** indicates $p < 0.001$.

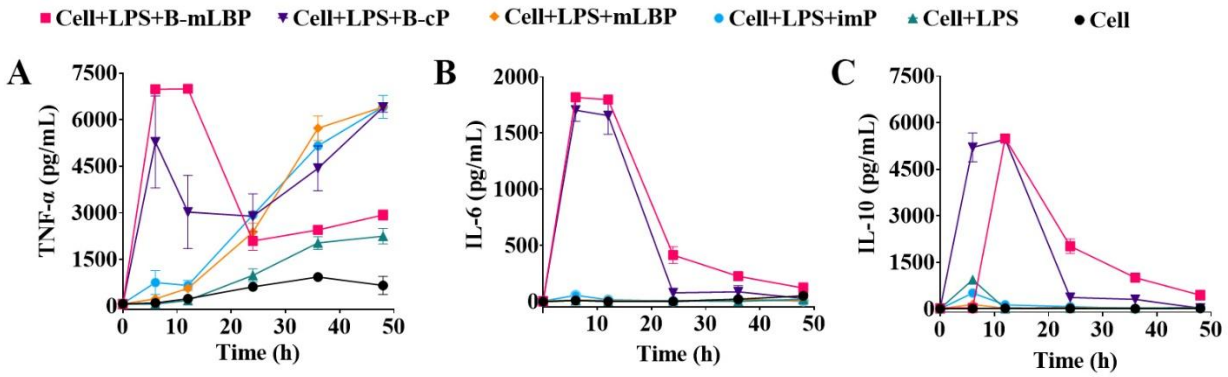

Figure S10. Regulatory effect of synthetic peptides on inflammation. Quantitative detection of TNF-α (A), IL-6 (B), and IL-10 (C) secreted by macrophages upon stimulation by LPS or synthetic peptides over time by ELISA. Macrophages only were used as a negative control group, and macrophages incubated with LPS were used as a positive control group.

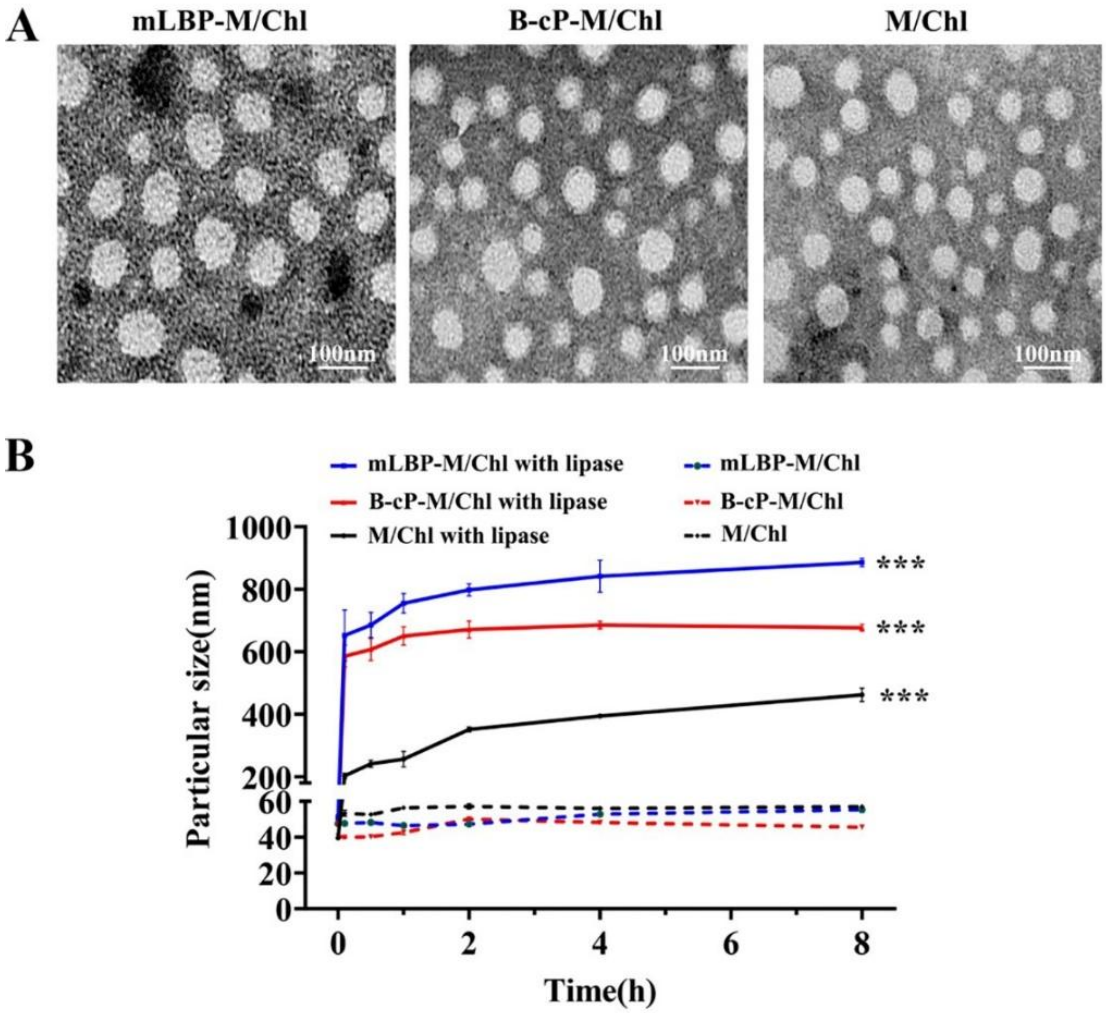

Figure S11. Chl-loaded micelles and their responsivity to lipase. (A) The TEM image of mLBP-M/Chl, B-cP-M/Chl, and M/Chl. (B) The particle size distribution of mLBP-M/Chl, B-cP-M/Chl, and M/Chl at 37°C with time in the presence or absence of 30 U/mL lipase. *** indicates $p < 0.001$ (The same micelles in the presence of lipase versus those in the absence of lipase).

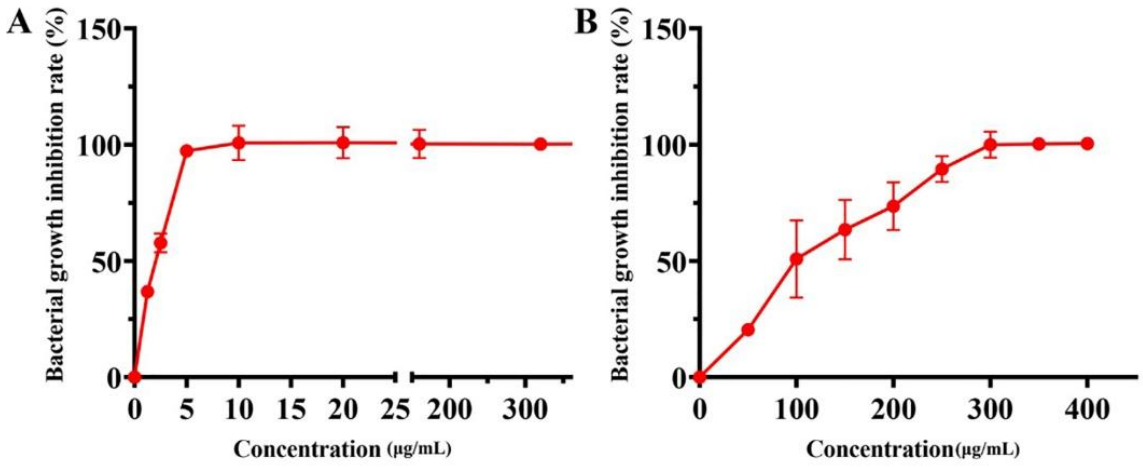

Figure S12. The chloramphenicol resistance of *S.typhimurium* after induction. (A) The minimum inhibitory concentration (MIC) of chloramphenicol against *S.typhimurium* before induction is 5 μg/mL. (B) The MIC of chloramphenicol against *S.typhimurium* after induction is 300 μg/mL.

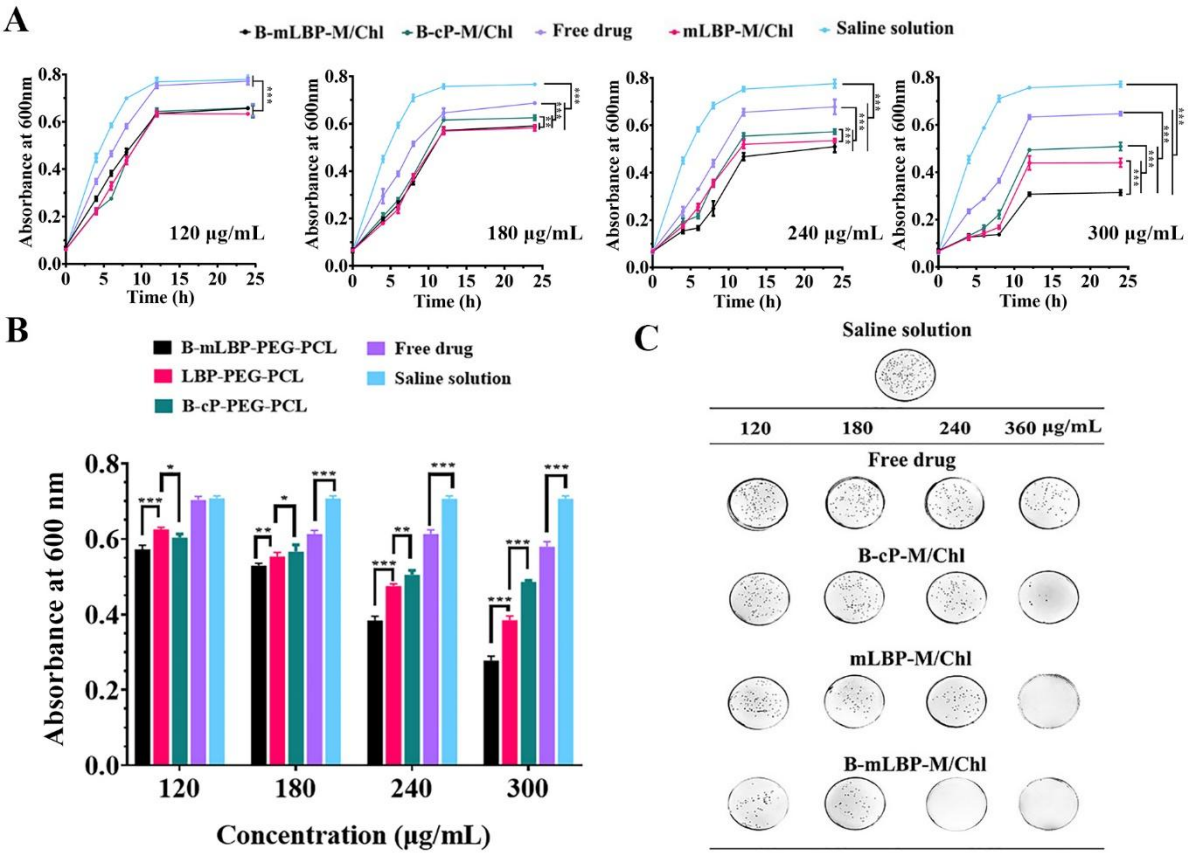

Figure S13. *In vitro* anti-resistant bacteria activity of different micelles. (A) The growth curve of the bacteria incubated with different concentrations of B-mLBP-M/Chl, mLBP-M/Chl, B-cP-M/Chl, or free drug at 37°C

during 24 h, respectively. (B) The concentration (OD_{600}) of residual bacteria at the endpoint of incubation (12 h) with different concentrations of B-mLBP-M/Chl, mLBP-M/Chl, B-cP-M/Chl, or free drug at 37°C. (C) Inoculation of the residue bacteria at the incubation endpoint for 18 h by the spread plate method. * indicates $p < 0.05$; ** indicates $p < 0.01$; *** indicates $p < 0.001$.

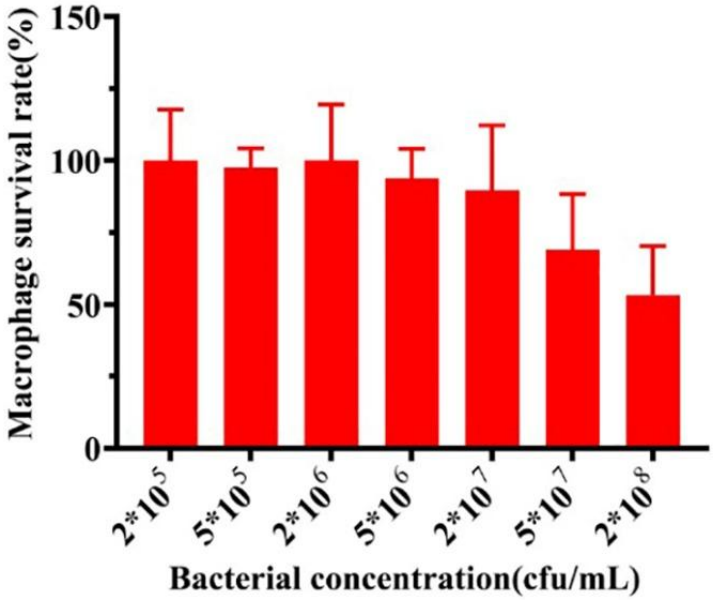

Figure S14. Screening of safe concentration for co-culture of bacteria with macrophages.

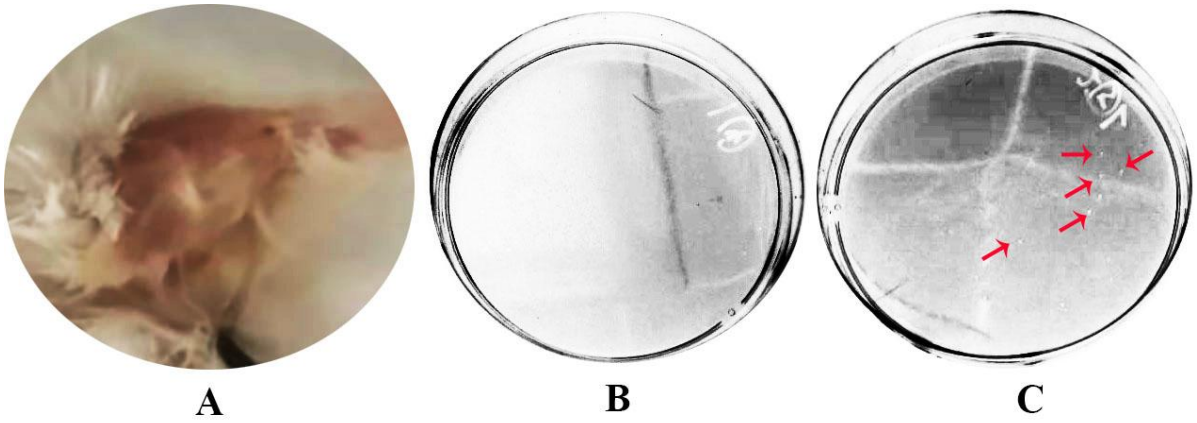

Figure S15. Judgment of localized *S.typhimurium* infection model of thigh. (A). The mice showed white pus in their thighs on the 7th day after infection. (B). *S.typhimurium* did not show in blood of mice with local infection. (C). There were *S.typhimurium* colonies in the cultured homogenate of infected thigh muscle.

References

1 Y. Zhao, H. Gao, J. H. He, C. P. Jiang, J. Lu, W. L. Zhang, H. Yang and J. P. Liu, *Journal of Controlled Release*, 2018, **283**, 241-260.

2 M. G. Coppolino, C. Kong, M. Mohtashami, A. D. Schreiber, J. H. Brumell, B. B. Finlay, S. Grinstein and W. S. Trimble, *Journal of Biological Chemistry*, 2001, **276** (7), 4772-4780.

3 J. Belmans, M. Van Woensel, B. Creyns, J. Dejaegher, D. M. Bullens and S. W. Van Gool, *Scientific Reports*, 2017, **7** (1), 97-109.

4 C. Wenisch, B. Parschalk, A. Weiss, K. Zedwitz-Liebenstein and W. Graninger, *Clinical & Diagnostic Laboratory Immunology*, 1996, **3** (4), 423-428.

5 V. Chandra, E. Bhagyaraj, R. Nanduri, N. Ahuja and P. Gupta, *Autophagy*, 2015, **11** (11), 1987-1997.

6 Z. Xu, G. S. Qian, Q. Li, Q. J. Feng, G. M. Wu and K. L. Li, *Inflamm. res.,* 2009, **58** (1), 45-53.